Altered evoked low-frequency connectivity from SI to ACC following nerve injury in rats

Tøttrup, Lea; Atashzar, S Farokh; Farina, Dario; Kamavuako, Ernest Nlandu; Jensen, Winnie

Published in:
Journal of Neural Engineering

DOI (link to publication from Publisher):
10.1088/1741-2552/abfeb9

Publication date:
2021

Document Version
Accepted author manuscript, peer reviewed version

Altered evoked low-frequency connectivity from SI to ACC following nerve injury in rats

To cite this article before publication: Lea Tøttrup *et al* 2021 *J. Neural Eng.* in press https://doi.org/10.1088/1741-2552/abfeb9

IOP Publishing Journal of Neural Engineering
Journal of Neural Engineering **XX** (XXXX) XXXXXX https://doi.org/XXXX/XXXX

Altered evoked low-frequency connectivity from SI to ACC following nerve injury in rats

Lea Tøttrup[1], S. Farokh Atashzar[2,3], Dario Farina[2], Ernest Nlandu Kamavuako[4,5], Winnie Jensen[1]
[1]Center for Neuroplasticity and Pain (CNAP), Department of Health Science and Technology, Aalborg University, Aalborg, Denmark.
[2]Department of Bioengineering, Imperial College London, UK
[3]Tandon School of Engineering, New York University, USA
[4]Department of Engineering, King's College London, United Kingdom
[5]Université de Kindu, Faculté de Médecine, Département des Sciences de base, Maniema, DR Congo

E-mail: ltj@hst.aau.dk

Received 11-12-2020
Accepted for publication xxxxxx
Published xxxxxx

Abstract

Objective. Despite decades of research on central processing of pain, there are still several unanswered questions, in particular regarding the brain regions that may contribute to this alerting sensation. Since it is generally accepted that more than one cortical area is responsible for pain processing, there is an increasing focus on the interaction between areas known to be involved. *Approach*. In this study, we aimed to investigate the bidirectional information flow from the primary somatosensory cortex (SI) to the anterior cingulate cortex (ACC) in an animal model of neuropathic pain.19 rats (nine controls and ten intervention) had an intracortical electrode implanted with six pins in SI and six pins in ACC, and a cuff stimulation electrode around the sciatic nerve. The intervention rats were subjected to the spared nerve injury after baseline recordings. Electrical stimulation at three intensities of both noxious and non-noxious stimulation was used to record electrically evoked cortical potentials. To investigate information flow, two connectivity measures were used: phase lag index (PLI) and granger prediction (GP). The rats were anesthetized during the entire study. *Main results*. Immediately after the intervention (<5 minutes after intervention), the high frequency (γ and γ+) PLI was significantly decreased compared to controls. In the last recording cycle (3-4 hours after intervention), the GP increased consistently in the intervention group. Peripheral nerve injury, as a model of neuropathic pain, resulted in an immediate decrease in information flow between SI and ACC, possibly due to decreased sensory input from the injured nerve. Hours after injury, the connectivity between SI and ACC increased, likely indicating hypersensitivity of this pathway. *Significance*. We have shown that both a directed and non-directed connectivity between SI and ACC approach can be used to show the acute changes resulting from the SNI model.

Keywords: Granger Prediction, Functional Connectivity Analysis, Spared Nerve Injury, Animal Model of Pain

1. Introduction

Neuropathic pain is estimated to affect up to 10 % of the general population [1]. It is largely unmanaged and therefore has a substantial negative effect on the quality of life [2,3]. Despite years of extensive research, many aspects of pain processing are still not understood. It is, however, known that pain is a complex experience involving several non-specific cortical and sub-cortical areas and pathways.

Anterior cingulate cortex (ACC) and the primary somatosensory cortex (SI) are involved in different aspects of pain processing. SI was conventionally believed to be part of the sensory-discriminatory system and ACC as a part of the cognitive-affective system [4–7]. While this view of specific roles of SI and ACC is outdated and simplified, both seem to be involved in the processing of pain and nociception [4].

The interactions between neurons in the same and different cortical areas occur through oscillatory activity, which is a mix of inhibitory and excitatory mechanisms [8]. Similar to the

non-specific pain-related activation of cortical areas, no pain-specific frequency domain activation has been found [8]. Nonetheless, oscillations in specific frequency bands have been linked to pain processing [8]. Oscillations in both SI and ACC have been found to be altered in animal models of pain, both in low (theta, delta, alpha) [9,10], and high (gamma, high gamma) [9–12] frequencies. In addition to the study of oscillatory activity in individual areas, the interactions between separate areas can be studied through connectivity measures.

Even with significantly increased activation of one or more areas, the interaction between areas is not necessarily affected by pain, as it was shown in a model of Complete Freund's Adjuvant (CFA) [13]. However, changes in connectivity but not in oscillatory activity in one area have also been found 28 days after intervention in an animal model of osteoarthritis [14]. Several studies have shown changes in cortical connectivity in animal models of pain, both during resting state and using evoked potentials. Resting-state connectivity between SI and prefrontal cortex was found to increase days after chronic constriction injury [13]. Resting-state connectivity is either unchanged or decreased between SI and thalamus minutes and days after injury [11,15]. Along the same line of research, evoked connectivity between ACC and amygdala was found to decrease in a model of inflammatory bowel disease (visceral pain) [16]. Even though a model of short term inflammatory pain showed functional cortical changes hours after the intervention [17,18], it has not been investigated whether this is also the case for long-lasting models of neuropathic pain. The interaction of evoked potentials between SI and ACC, however, seems to be strengthened during a state of inflammatory pain [17–19], indicating that this specific pathway is important for the processing of pain. If cortical changes can be shown in the hours following a model of neuropathic pain, similar to a model of inflammatory pain, then the nerve injury model of pain would cause neural changes faster than previously expected.

The interactions between SI and ACC are known to be affected by both noxious stimuli and a model of inflammatory pain, as observed in previous studies [10,12,17,20]. Additionally, the interaction between these two areas and several other areas are affected in models of inflammatory and neuropathic pain. It is not known how the SI-ACC interactions are affected in the hours after a model of neuropathic pain. This study aimed to evoke the cortical interaction between SI and ACC and investigate the changes in this pathway as a result of a peripheral nerve injury. We hypothesized that the cortical connectivity from SI to ACC would increase following an animal model of pain.

2. Methods

The procedures used in this study were approved by the Danish Animal Experiment inspectorate (J. no.: 2016-15-0201-00884). The rats used in this study were albino Sprague Dawley rats from Taconics Europe. They were kept caged with 2-3 rats in each in a room with a 12:12 light/dark cycle and controlled temperature and humidity. Food and water were supplied ad libitum. At arrival, the rats had a two-week acclimatization quarantine. Following these two weeks, the rats were handled by the experimenter several times where the animals also were accustomed to the anesthesia induction chamber. The purpose of the handling was to minimize a potential stress response on the day of the experiment.

2.1 Spared nerve injury model

The spared nerve injury (SNI) model [21] is an animal model of neuropathic pain. This model consists of a nerve injury by transection of the tibial and common peroneal branches of the sciatic nerve in the hind limb. The third branch, the sural branch, of the sciatic nerve is left intact, which in this study serves two purposes. When leaving part of the nerve intact, some sensory input is preserved, prevention self-mutilation in future recovery studies, and to be able to stimulate the nerve to evoke cortical sensory responses in this study.

Behavioral signs of neuropathic pain have previously been used to validate the spared nerve injury model as robust and reliable [22–24]. The model results in e.g. mechanical and thermal sensitivity [21,25], symptoms mimicking neuropathic pain in humans [26].

2.2 Experimental setup

Nine rats were randomly assigned to a control group (weight: 333-417 g, age: 10-11 weeks) and ten rats to an intervention group (weight: 332-398 g, age: 9-12 weeks). The only difference between the control and intervention groups was the ligation and transection of the nerve to implement the SNI model. All rats were anesthetized at the beginning of the experiment and kept anesthetized until the experiment ended with a lethal intracardial injection of pentobarbital. The initial anesthesia was supplied into an induction chamber with 4 % isoflurane in medical grade oxygen (99 %) at a flow rate of 2 L/min. After a few minutes when no movements could be detected, the rats were moved to a mask in a stereotaxic frame (KOPF®) where the head could be kept steady using ear bars. The anesthesia was continuously supplied through the mask and regulated based on physiological parameters (heart and breath rate). It was between 1-3 % throughout the remaining experiment.

2.3 Surgical procedures

Intracortical signals were recorded with a multi-electrode array (MEA, AlphaOmega, 0.5 mm between pins, tungsten

needles, shank diameter without insulation: 75 µm). A cut was made through the skin on top of the head of the rats and a craniotomy was performed, resulting in a 6*4 mm hole on the left side of the midline. The dura was carefully removed, and a MEA with 12 pins (6 in ACC and 6 in SI) was inserted. The placements of the pins were based on Paxinox rat atlas [27], and previous research [28,29] using bregma and the midline as landmarks, and were as follows; SI: AP -1.5 to -2.0 mm, ML 1.0 to 3.0 mm, DV 1.4 mm, ACC: AP 0.5 to 2.0 mm, ML 0.5 to 1.0 mm, DV 2.7 mm. The electrode was inserted quickly using a micromanipulator to a depth further than the desired target depth and retracted to avoid dimpling of the brain.

In addition to the insertion of the cortical electrode, a bipolar cuff electrode (length = 10 mm, diameter = 2 mm, [30]) was inserted around the sciatic nerve in the leg to evoke cortical potentials. A cut was made through the skin and the biceps femoris was separated enough to place the cuff electrode placed around the sciatic nerve above the branches. The cuff was secured with a suture (4-0 silk). Sutures were also placed around the tibial and common peroneal branches as preparation for the SNI procedure.

2.4 Data recording

To evoke intracortical potentials, electrical stimuli (2 Hz, 0.1 ms pulse width, square pulses, Multi-channel stimulus II and Grass SD9 stimulator) with varying intensities were used. The stimulation intensities were relative to each individual rat's movement threshold. The movement threshold was found by recording the electromyographic signal using an intramuscular needle electrode. The purpose of applying the three different intensities was to be able to study the evoked potential to activation of different types of peripheral fibers. The intensities were based on Chang et al. (2001) that assessed and identified the electrical peripheral stimulation intensities necessary to activate Aβ, Aδ, and C-fibers [31]. Stimulation intensities were at 2, 4, and 10x movement threshold (low, medium, and high). At 2x movement threshold, only some Aβ fibers are assumed to be activated. When the stimulation is increased to 4x movement threshold, a larger portion of Aβ fibers are activated, while few or none Aδ fibers are activated, and it is thereby still believed to be a non-noxious stimulation. At 10x movement threshold, around 70 % of the Aδ fibers are activated in addition to all or most of the Aβ fibers [31].

Each recording of intracortical signals consisted of 30 s resting state and 1 min of electrical stimulation (sampling frequency 24,414, PZ5 neurodigitizer and PZ2 BioAmp Processor, Tucker-Davis Technologies), resulting in 120 stimuli pr. recording. The recordings were carried out in cycles with first a low stimuli intensity recording, then high-intensity stimuli, and lastly medium intensity stimuli recording with a 30 min break between all recordings except for the first recording after SNI which was performed immediately after. Instead of the SNI procedure, the control group was subjected to a 15 min wait period, which was the approximate time to took to perform the SNI procedure. One cycle or three recordings were done before SNI or with and used as a baseline, and three cycles after SNI, resulting in 3 baselines and 9 post-baseline recordings in total.

2.5 Data processing

All data processing was done in Matlab R2019b (The Mathworks Inc., USA). The intracortical recordings were pre-processed by a digital bandpass filter (2nd order Butterworth, cut off 1-200 Hz) and a sequence of notch filters (2nd order Butterworth, at 50 Hz, 100 Hz, 150 Hz with the width of cut off +/- 1 Hz) to remove the power line noise. The channels were visually inspected to exclude channels with only noise (30/2736 channels in total from all recordings). Most removed channels were due to a faulty pin in the electrode in two of the rats (in total 24). To minimize the effect of the volume conductor and to maximize spatial resolution, a double differential operator was applied on the signal space from each area's six electrodes and used as two channels in the following analysis (see Figure 1). The double differential signals were calculated in two steps, first by finding the difference between the two middle pins (black dots in Figure 1, multiplied with 2) in each area and the four outer pins (grey dots in Figure 1, multiplied with -1), and second by finding the difference between the two signals from step 1 (black dot and grey dot in figure 1), the whole equation being $SI_{activity} = [(-1 * s_1 + 2 * s_2 - 1 * s_3) - (-1 * s_4 + 2 * s_5 - 1 * s_6)]$ where s_1-s_6 is the signal from each pin in SI.

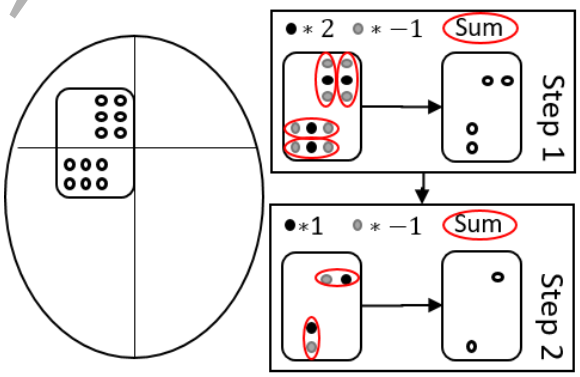

Figure 1: Top view of electrode placement. The vertical line is the midline on the scull and the horizontal line is Bregma. The boxes on the right side visualizes how the double differential signals were calculated in two steps resulting in one signal from each area.

The signals were filtered (2nd order Butterworth) in the classic frequency bands known from EEG analysis (δ: 0.5-4 Hz, θ: 4-8 Hz, α: 8-13 Hz, β: 14-40 Hz, (low)-γ: 40-49 Hz, high-γ: 51-100 Hz, hereafter written and γ and high-γ) [32] and Hilbert transformed [33]. From the Hilbert transform, the analytical signal is extracted and was used to calculate

connectivity between SI and ACC. When calculating the analytical signal, the imaginary part is extracted, found by rotating the Fourier transform (FFT), while keeping the real part of the signal [33]. Thereby both the amplitude and phase of the signal can be found. The functional connectivity between SI and ACC was estimated by calculating phase lag index (PLI) and Granger prediction (GP). It is not clear whether the use of different approaches is the cause for heterogeneous findings in previous research attempting to study connectivity; therefore, we eploy both a non-directed and a directed connectivty approach (PLI and GP, respectively).

2.6 Phase lag index

The functional connectivity between SI and ACC was assessed using the PLI. Its definition is based on the power spectral density. With respect to the more traditional coherence function, PLI is less sensitive to the effect of the volume conduction and to outliers in the data [33]. PLI is a number between 0 and 1, where 0 indicates no connectivity and 1 indicated strong connectivity. PLI is calculated using the following equation [33]:

$$PLI_{xy} = \left| n^{-1} \sum_{t=1}^{n} sgn(imag(S_{xyt})) \right|$$

Where *sgn* is the sign of the imaginary part of the cross-spectral density S_{xyt} between SI and ACC, defined as:

$$S_{xyt} = \hat{X}(t) \times \hat{Y}(t)^{*}$$

Where $\hat{X}$ and $\hat{Y}$ are the analytic signals from SI and ACC. In the calculation of the analytic signal, a complex component is added to each sample of a time series. PLI was calculated for each recording as an average across epochs. Each epoch consisted of the 500 ms following a stimuli (in total 120 epochs in each recording). PLI is an index for each frequency within a predefined frequency spectrum or a number of specific frequencies. In this study PLI was calculated in the above mentioned frequency bands (δ, θ, α, β, γ, and high-γ).

2.7 Granger prediction

GP (also known as Granger causality [34]), is a method to quantify the influence (seen as predictability) one has one another and vice versa. The method has been used for many years in neuroscience [35,36]. The term GP will be used in this paper, as the measures do not determine causality but merely whether previous values from one signal can better predict current values from another signal than the other signal alone [33].

All calculations were made using the Multi-variate Granger Causality Matlab toolbox [36,37]. The data were down-sampled to 1000 Hz to optimize computational processing time. The calculation was made across all frequency bands (1-200 Hz). GP is based on autoregression (AR), and firstly, the model order was estimated using Bayes information criteria (BIC), which is better than Akaike information criterion for data with many trials [33]. Secondly, the univariate AR, which is a model predicting current samples based on previous samples from the same cortical area, and the bivariate AR, which is a model predicting current samples from one cortical area based on samples from the same and another cortical area were calculated. When estimating the model order, the error from fitting the bivariate AR is used [33]. The univariate and bivariate ARs for one cortical area are calculated using the following equations [33]:

$$X_t = \sum_{n=1}^{k} a_n X_{t-n} + e_{xt}$$

$$X_t = \sum_{n=1}^{k} a_n X_{t-n} + \sum_{n=1}^{k} b_n Y_{t-n} + e_{xt}$$

Where X is the signal from one area, and Y is the signal from another. k is the order of the AR, a is a weighting term, and e is the error or residual that cannot be predicted from previous samples. The same calculations are made for Y.

The AR was transformed into spectral causality to calculate the GP in the frequency domain using the fast Fourier transform [37]. The following calculations are based on the transformed (spectral) ARs. The GP is calculated as the difference in error variance between the univariate and bivariate AR. This means that if the AR did not change when including previous samples from another area, the difference in variance and thereby connectivity would be close to zero.

The GP is calculated using the following equation:

$$Granger\ prediction = \ln\left(\frac{var(e_x)}{var(e_{xy})}\right)$$

Where ln is the natural logarithm, e_x is the error from the univariate AR for X and e_{xy} is the error from the bivariate AR for X. The same calculation is made for Y.

2.8 Statistical analysis

For both visualization and statistical analysis, the z-score (each data point was subtracted by the mean of all baseline recordings and divided with the standard deviation of the baseline of the same intensity stimulation) was used to normalize the data. All statistical analyses were made in SPSS 26. The PLI and GP across samples were quantified as area-under-the-curve (AUC) and the difference between recordings was analyzed used repeated-measures ANOVA. PLI was analyzed with one between-subject factor (groups, [intervention, control]) and two within-subject factors (time, [baseline, 1st, 2nd, 3rd cycle], intensity, [low, medium, high intensity]). The GP was analyzed using the same factors and one additional within-subject factor (direction of activity, [ACC→SI, SI→ACC]). Multiple comparisons for each frequency were made in case of overall difference across all frequencies and Bonferroni corrected.

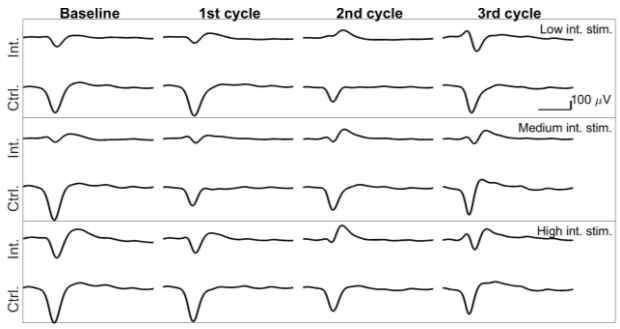

Figure 4: Electrically evoked cortical potentials (100 ms) in the primary somatosensory cortex. Each potential is the average of the potentials from all intervention (int.) and control (ctrl.) rats in every other row. The intervention was done between baseline and 1st cycle.

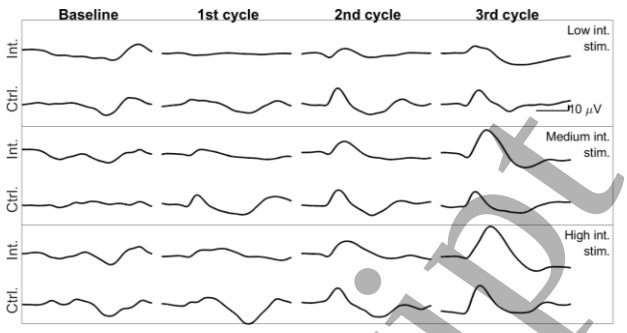

Figure 3: Electrically evoked cortical potentials (100 ms) in the anterior cingulate cortex. Each potential is the average of the potentials from all intervention (int.) and control (ctrl.) rats in every other row. The intervention was done between baseline and 1st cycle.

3. Results

From the intracortical data, functional connectivity was investigated. The electrically evoked cortical potentials (EECP), averaged across all rats, are visualized in Figures 2 and 3 for SI and ACC, respectively.

The EECPs were found to be larger in SI with higher intensity stimuli (Figure 2, low vs. medium and high intensity). In the intervention group, a positive peak followed the larger negative peak hours following SNI. The EECP in ACC was larger at the last recordings, especially with medium and high-intensity stimuli in the intervention group (figure 3).

3.1 Phase lag index

The results from the statistical analysis showed that the PLI first decreased over time for both groups, followed by an increase in the last recording ($F_{1.84,1.83}$=3.22, p=0.057, η_p^2=0.16). This was, however, only the case in some frequency bands as the development in connectivity differed between frequency bands ($F_{4.39,74.60}$=3.58, p=0.008, η_p^2=15.69). The PLI in the α-band kept increasing over time, whereas the activity in the remaining frequency bands decreased in the first two recordings following SNI and increased at the last

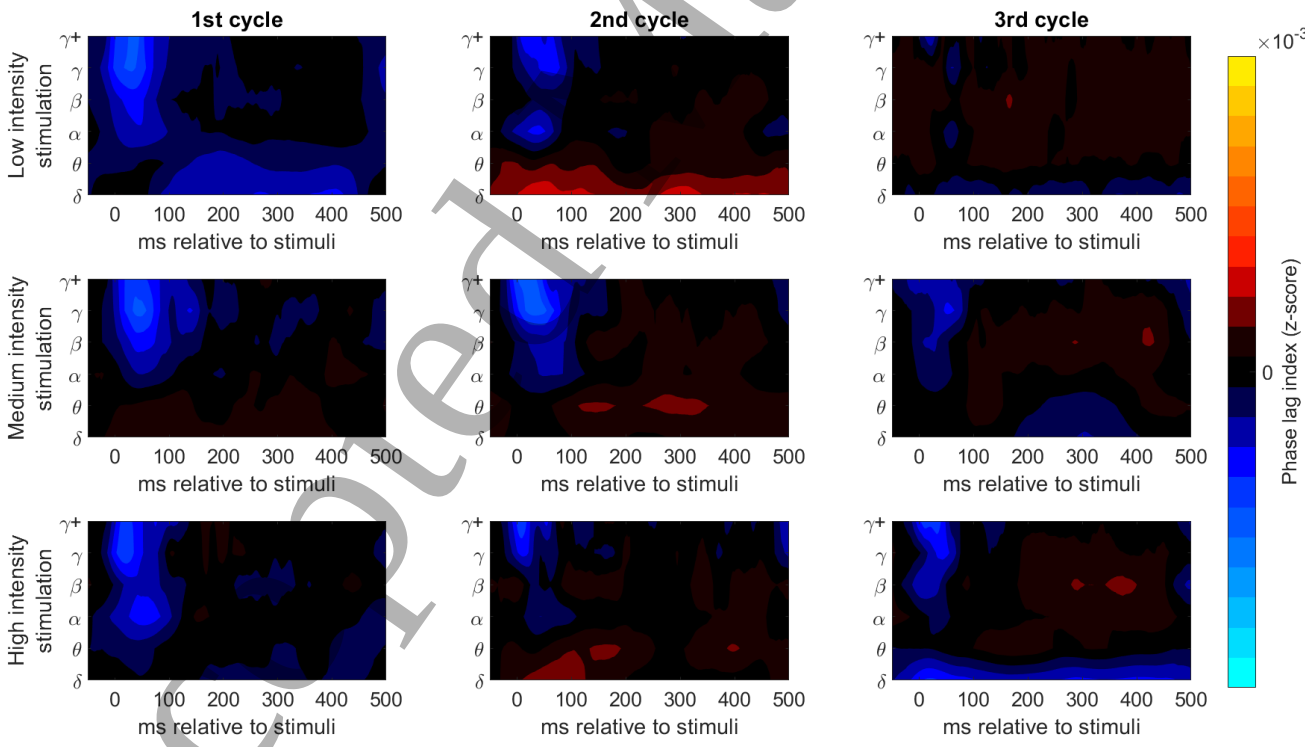

Figure 2: Time-frequency analysis across epochs for phase lag index. PLI is extrapolated between frequency bands. The colors represent the difference in PLI between intervention and control group. Yellow and red colors indicate higher PLI in the intervention group, and blue colors higher PLI in the control group.

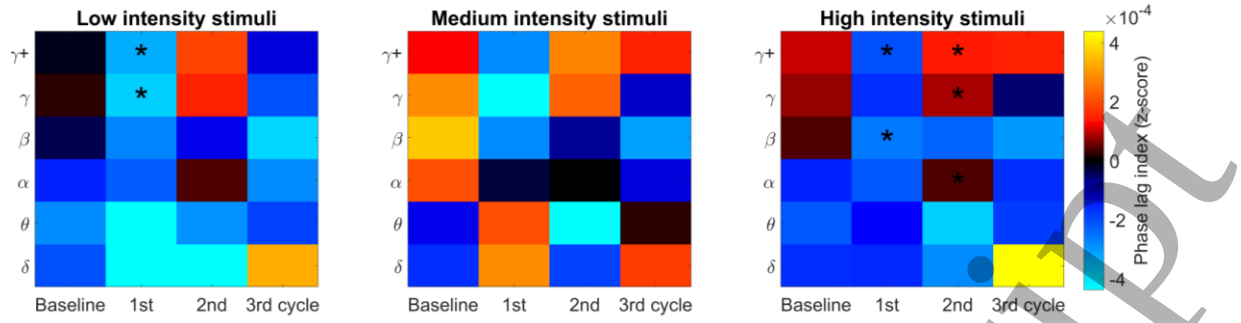

Figure 5: PLI difference between intervention and control group at each recording (average of the 500 ms epoch). Yellow and red colors indicate higher PLI in the intervention group and blue colors higher PLI in the control group. *Significant difference between groups ($p<0.05$) after Bonferroni correction.

recording to a level close to the baseline. PLI was higher with higher intensity electrical stimuli ($F_{2,34}=3.51$, $p=0.041$, $\eta_p^2=0.17$). From the time-frequency visualization (Figure 4) we see that the difference between groups was most pronounced within the first 100 ms after stimuli in the first recording after SNI. At this specific time, the PLI between SI and ACC in the intervention group was decreased compared to the control group. Further, a non-statically significant increase in delta band PLI was observed in the intervention group duing low intensity stimulation. In the last recording hours after SNI, the longer response in PLI (>100 ms) was increased in the intervention group when using high-intensity stimulation.

When analyzing the average PLI in the 500 ms epochs, the PLI in the intervention group significantly decreased (compared to controls) in the γ and high γ PLI at the first recording after SNI when using low and high-intensity stimulation (Figure 5, p = 0.008-0.014). With high-intensity stimuli, the PLI was significantly decreased in the first recording after SNI in the beta and high gamma bands (p = 0.021-0.047) and increased in the second recording in the gamma and high gamma bands (p = 0.034-0.041) compared to controls. This was a general trend, as the PLI in the first recording following SNI was decreased in the intervention group compared to controls. In general, the average higher frequency PLI was increased for the intervention group at later recordings. Using medium intensity stimuli, the two groups differed more at baseline than during low and high-intensity stimuli. This difference was not statistically significant.

3.2 Granger prediction

The GP values increased over time (figure 6, $F_{1.77,30.17}=6.87$, $p=0.005$, $\eta_p^2=0.29$). There was, however, no statistically significant difference between recording during low, medium, and high-intensity stimulation ($F_{1.36,23.09}=0.47$, $p=0.56$, $\eta_p^2=0.027$). The GP values were significantly different in the control and intervention group ($F_{1,17}=16.60$, $p=0.001$, $\eta_p^2=0.49$). The largest increase in GP was observed in the lower frequencies.

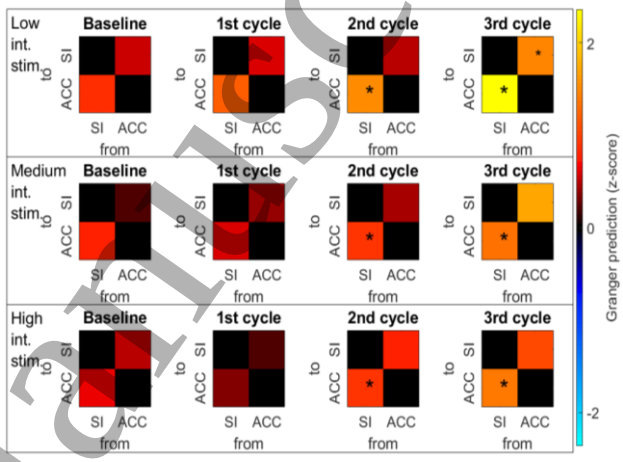

Figure 6: Difference between intervention and control group in GP across frequencies (z-scored AUC, 1-100 Hz). Red and yellow colors indicate larger GP values in the intervention group and blue colors indicate larger GP values in the control group. * indicates statistical significance between the two groups ($p<0.05$, Bonferroni corrected.)

When comparing GP between control and intervention group (figure 6), the z-scored AUC values were significantly larger in the intervention group during the 2nd and 3rd recording cycle using all three stimulation intensities from SI to ACC ($p=0.013$-0.041). The differences were analyzed in a post hoc analysis which showed the difference being the the low (δ, θ) and middle (α, β) frequency bands (figure 7). Furthermore, the GP between ACC and SI was increased in intervention rats compared to controls in the last recording cycle when using low-intensity stimulation ($p=0.047$). There was an increased GP already at baseline in the intervention group (not statistically significant).

4. Discussion

The main finding of this study is that low-frequency GP is increased from SI to ACC hours following nerve injury in an animal model of neuropathic pain. This indicates that the SNI model influences electrically evoked cortical connectivity already hours after the intervention. The connectivity, quantified as PLI between EECP from SI and ACC changed

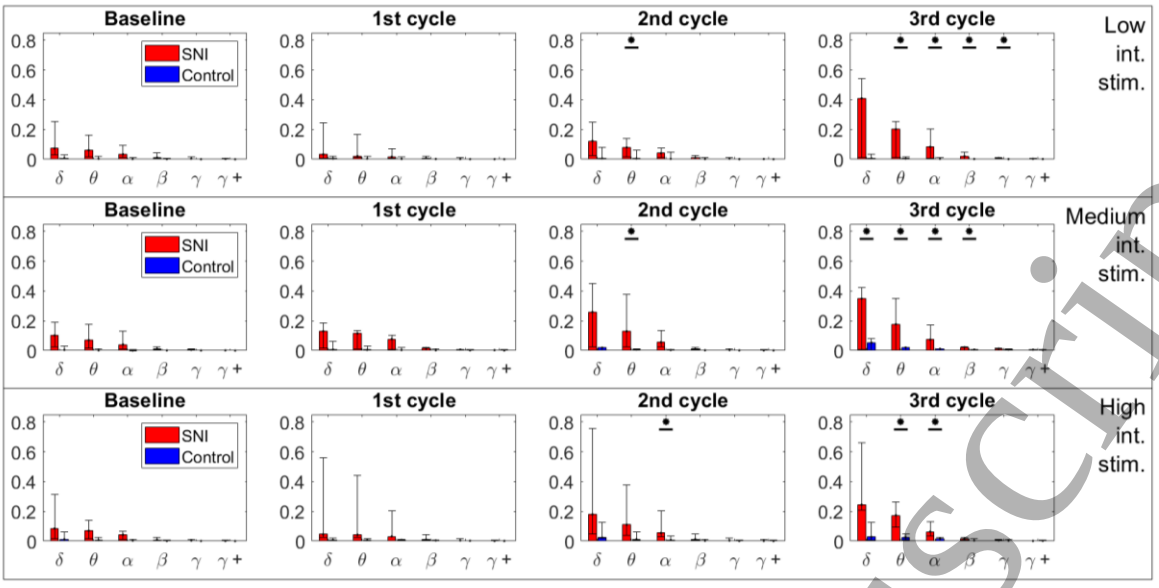

Figure 5: Median GP (SI→ACC) with the 25th and 75th quartile for each frequency (δ-γ+) for the SNI (red) and control (blue) group for each time point (horizontal) and stimulation intensity (vertical). * indicate statistically significant difference between groups, Bonferroni adjusted.

significantly following a peripheral nerve injury. PLI in high-frequency bands was decreased immediately after injury, followed by an increase. A significant increase in the communication from SI to ACC, quantified as GP, developed over time and was present in the last two recording cycles using both low, medium, and high-intensity stimulation.

4.1 Decreased short term PLI

Previous research has found increased, mostly at high frequencies, oscillatory activity in either SI, ACC, or both [10,12,13,18,28,38] shortly after intervention with an animal model of pain. Increases in oscillatory activity in one or more cortical areas do not equal changes in connectivity which is why resting-state connectivity is decreased in the minutes or hours following and capsaicin [11] and days or weeks after peripheral nerve injury [11,15]. The minutes and hours following SNI have, however, not been previously investigated. This was done in the present study, using intracortical activity from SI and ACC following SNI. During pain induced with a noxious laser stimulation, the cortical activation of SI and ACC are increasingly correlated [12]. This may be an indication of connectivity being increased between SI and ACC during evoked potentials. Correlation, however, cannot be used to investigate directional connections, which has been done in this study. There are two approaches to investigating neuropathic pain in animals. In the acute time domain, evoked potentials to noxious stimuli are investigated and in the prolonged/chronic (days and weeks) time domain, models of neuropathic pain are used. It is difficult to predict if the chronic models result in acute cortical changes or if the protocol used in this study, i.e. evoked potentials following a model of neuropathic pain in the acute time domain, results in functional connectivity more similar to noxious stimuli studies. It is important to take into account that the nerve subjected to injury is the same that is being stimulated to evoke cortical potentials. The decreased input from the periphery may influence the connectivity and could be the cause of the initial decrease. Connectivity is enhanced between ACC and other cortical areas but not between ACC and SI immediately after SNI [28].

A study using a model of visceral pain showed prolonged decreased PLI five days after intervention evoked by cortical stimulation [16]. This was shown in the theta band, without investigating other frequencies. Without investigating the development in PLI before 5 days, it is hard to know what happens within a time frame comparable to the one in the present study. In human studies, resting-state connectivity has likewise been found to be decreased in chronic pain patients [39]. During stimulation, one study found that PLI increased when provoking pain in osteoarthritis patients [40]. Due to the time frame of the present study, it is not known how PLI develops during the first days following a model of pain.

4.2 Increased SI→ACC information flow hours after SNI

The GP in the present study was found to be consistently increased in the 2nd and 3rd recording cycle from SI to ACC and the last recordings cycle during low-intensity stimulation from ACC to SI. This is also somewhat consistent with the increased low-frequency (δ-band) PLI in the 2nd recording during low intensity stimulation in the intervention group (figure 4), although only GP in this specific recording was only different between groups in the θ-band. This was not different between groups ($p < 0.05$) however. GP has previously been shown to increase in both directions (SI to

ACC and ACC to SI) in a model of complete Freund's adjuvant (CFA) between SI and ACC [17]. The findings by Guo et al. (2020) support the results of the present study even though we only found consistently increased GP from SI to ACC. The timeline in Guo et al. (2020) is not fully specified with respect to time between the injection of CFA and first recording, but it seems that the results are mostly comparable to the first cycle of recordings in the present study. No statistically significant changes in GP were found in the first cycle of recordings, which indicates that the effect of the SNI model is slower than the effect of CFA.

A constant, not-injury related information flow from SI to ACC may be present, also before the injury and in the control group and with the injury possibly causing a sustained hypersensitive state, this information flow could be increased, as shown previously [18,19,41]. High-frequency oscillations, such as in the gamma band, could be an indication of a hyperactive state, given that the oscillations are an expression of groups of neurons exciting or inhibiting other neurons, and higher frequency means faster oscillatory interactions. However, for specific frequency bands to increase in an electrophysiological recording, the neurons' activity needs to be synchronized. Even though previous research in both human pain patients and animal models of pain has been focused on gamma oscillations [9,10,42–44], lower-frequency oscillations have also been related to pain in animal models [8–12], similar to what was found in this study.

4.3 Limitations

In this study, all recordings were performed under isoflurane anesthesia, which limits the possibility of supporting the results with behavioral measures. Previous studies have shown that the SNI model results in pain-indicating behavior and that rats are showing symptoms corresponding to neuropathic pain patients [45–47].

When studying anesthetized animals, type and level of anesthesia is always a limitation. It has previously been shown that increasing levels of anesthesia results in more burst suppression of spontaneous cortical activity [48,49]. However, it was also shown that the response to noxious electrical stimulation was still present during isoflurane [48]. Additionally, both the control and intervention groups were anesthetized during the experiment and subjected to the same stimuli, so any effects on the EEVP due to the anesthetic level should affect both groups.

Conclusions regarding the cortical areas' influence on each other must be made with caution. Effective connectivity predicts an association between areas but it cannot rule out the possibility that a third area affects both areas and thereby that the interaction is not direct.

4.4 Conclusions

We investigated the immediate (minutes) and sustained (hours) response to a peripheral nerve injury (SNI) in anesthetized rats to assess whether this model of neuropathic pain resulted in short-term changes similar to the long-term changes shown in previous literature. EEVP used to evaluate an intervention by the SNI model of neuropathic pain showed an immediate high-frequency decrease in PLI, possibly due to decreased peripheral input. This was followed by an increased high-frequency functional connectivity in addition to a low-frequency effective connectivity information flow from SI to ACC, either directly or through other areas. Knowing that changes occur only hours after injury and that a connectivity approach can show these changes, creates a shorter time window to be investigated in relation to the passage from acute to chronic pain. In the future, a similar approach might be used to show acute cortical changes possibly before other long-term somatosensory changes can be detected.

Acknowledgements

This work was funded by the Center for Neuroplasticity and Pain (CNAP). CNAP is supported by the Danish National Research Foundation (DNRF121)

References

[1] Scholz J, Finnerup N B, Attal N, Aziz Q, Baron R, Bennett M I, Benoliel R, Cohen M, Cruccu G, Davis K D, Evers S, First M, Giamberardino M A, Hansson P, Kaasa S, Korwisi B, Kosek E, Lavand'homme P, Nicholas M, Nurmikko T, Perrot S, Raja S N, Rice A S C, Rowbotham M C, Schug S, Simpson D M, Smith B H, Svensson P, Vlaeyen J W S, Wang S-J, Barke A, Rief W and Treede R-D 2019 The IASP classification of chronic pain for ICD-11 *Pain* **160** 53–9

[2] Beniczky S, Tajti J, Tímea Varga E and Vécsei L 2005 Evidence-based pharmacological treatment of neuropathic pain syndromes *J. Neural Transm.* **112** 735–49

[3] Mcnicol E D, Midbari A and Eisenberg E 2013 Opioids for neuropathic pain *Cochrane Database Syst. Rev.* **2017**

[4] Wiech K 2016 Deconstructing the sensation of pain: The influence of cognitive processes on pain perception *Science (80-.).* **354** 584–7

[5] DosSantos M F, Moura B de S and DaSilva A F 2017 Reward circuitry plasticity in pain perception and modulation *Front. Pharmacol.* **8** Article 790

[6] Treede R D, Kenshalo D R, Gracely R H and Jones A K P 1999 The cortical representation of pain *Pain* **79** 105–11

[7] Seifert F and Maihöfner C 2011 Functional and structural imaging of pain-induced neuroplasticity *Curr. Opin. Anaesthesiol.* **24** 515–23

[8] Ploner M, Sorg C and Gross J 2017 Brain Rhythms of Pain *Trends Cogn. Sci.* **21** 100–10

[9] Chen Z, Shen X, Huang L, Wu H and Zhang M 2018 Membrane potential synchrony of neurons in anterior cingulate cortex plays a pivotal role in generation of neuropathic pain *Sci. Rep.* **8** 1–10

[10] Xiao Z, Martinez E, Kulkarni P M, Zhang Q, Hou Q, Rosenberg D, Talay R, Shalot L, Zhou H, Wang J and Chen Z S 2019 Cortical pain processing in the rat anterior

cingulate cortex and primary somatosensory cortex *Front. Cell. Neurosci.* **13** 1–14

[11] LeBlanc B W, Lii T R, Silverman A E, Alleyne R T and Saab C Y 2014 Cortical theta is increased while thalamocortical coherence is decreased in rat models of acute and chronic pain *Pain* **155** 773–82

[12] Li X, Zhao Z, Ma J, Cui S, Yi M, Guo H and Wan Y 2017 Extracting Neural Oscillation Signatures of Laser-Induced Nociception in Pain-Related Regions in Rats *Front. Neural Circuits* **11** 1–11

[13] LeBlanc B W, Bowary P M, Chao Y-C, Lii T R and Saab C Y 2016 Electroencephalographic signatures of pain and analgesia in rats *Pain* **157** 2330–40

[14] Abaei M, Sagar D R, Stockley E G, Spicer C H, Prior M, Chapman V and Auer D P 2016 Neural correlates of hyperalgesia in the monosodium iodoacetate model of osteoarthritis pain *Mol. Pain* **12** 1–12

[15] Zippo A G, Valente M, Caramenti G C and Biella G E M 2016 The thalamo-cortical complex network correlates of chronic pain *Sci. Rep.* **6** 1–13

[16] Cao B, Wang J, Mu L, Poon D C H and Li Y 2016 Impairment of decision making associated with disruption of phase-locking in the anterior cingulate cortex in viscerally hypersensitive rats *Exp. Neurol.* **286** 21–31

[17] Guo X, Zhang Q, Singh A, Wang J and Chen Z S 2020 Granger causality analysis of rat cortical functional connectivity in pain *J. Neural Eng.* **17** 016050

[18] Tan L L, Oswald M J, Heinl C, Retana Romero O A, Kaushalya S K, Monyer H and Kuner R 2019 Gamma oscillations in somatosensory cortex recruit prefrontal and descending serotonergic pathways in aversion and nociception *Nat. Commun.* **10** 983

[19] Eto K, Wake H, Watanabe M, Ishibashi H, Noda M, Yanagawa Y and Nabekura J 2011 Inter-regional contribution of enhanced activity of the primary somatosensory cortex to the anterior cingulate cortex accelerates chronic pain behavior *J. Neurosci.* **31** 7631–6

[20] Song Y, Kemprecos H, Wang J and Chen Z 2019 A Predictive Coding Model for Evoked and Spontaneous Pain Perception *Annual International Conference of the IEEE Engineering in Medicine and Biology Society* (IEEE) pp 2964–7

[21] Decosterd I and Woolf C J 2000 Spared nerve injury: an animal model of persistent peripheral neuropathic pain *Pain* **87** 149–58

[22] Cardoso-Cruz H, Lima D and Galhardo V 2013 Impaired Spatial Memory Performance in a Rat Model of Neuropathic Pain Is Associated with Reduced Hippocampus-Prefrontal Cortex Connectivity *J. Neurosci.* **33** 2465–80

[23] Baliki M N, Chang P C, Baria A T, Centeno M V. and Apkarian A V. 2014 Resting-state functional reorganization of the rat limbic system following neuropathic injury *Sci. Rep.* **4** 1–11

[24] Campbell J N and Meyer R A 2006 Mechanisms of neuropathic pain *Neuron* **52** 77–92

[25] Xie W, Strong J A, Meij J T A, Zhang J-M and Yu L 2005 Neuropathic pain: Early spontaneous afferent activity is the trigger *Pain* **116** 243–56

[26] Seifert F and Maihöfner C 2009 Central mechanisms of experimental and chronic neuropathic pain: Findings from functional imaging studies *Cell. Mol. Life Sci.* **66** 375–90

[27] Paxinos G and Watson C 2007 *The rat brain in stereotaxic coordinates* (Elsevier Inc.)

[28] Chao T H, Chen J and Yen C 2018 Plasticity changes in forebrain activity and functional connectivity during neuropathic pain development in rats with sciatic spared nerve injury *Mol. Brain* **11** 55

[29] Han Y, Li N, Zeiler S R and Pelled G 2013 Peripheral nerve injury induces immediate increases in layer v neuronal activity *Neurorehabil. Neural Repair* **27** 664–72

[30] Haugland M 1996 Flexible method for fabrication of nerve cuff electrodes *18th Annual International Conference of the IEEE Engineering in Medicine and Biology* pp 359–60

[31] Chang C and Shyu B-C 2001 A fMRI study of brain activations during non-noxious and noxious electrical stimulation of the sciatic nerve of rats *Brain Res.* **897** 71–81

[32] Noachtar S, Binnie C, Ebersole J, Maugiére F, Sakamoto A and Westmoreland B 2004 A Glossary of Terms Most Commonly Used by Clinical Electroencephalographers and Proposal for the Report Form for the EEG Findings *Klin. Neurophysiol.* **35** 5–21

[33] Cohen M X 2014 *Analyzing Neural Time Series Data. Theory and Practice* (The MIT Press)

[34] Granger C W J 1969 Investigating Causal Relations by Econometric Models and Cross-spectral Methods *Econometrica* **37** 424

[35] Kamiński M, Ding M, Truccolo W A and Bressler S L 2001 Evaluating causal relations in neural systems: Granger causality, directed transfer function and statistical assessment of significance *Biol. Cybern.* **85** 145–57

[36] Seth A K 2010 A MATLAB toolbox for Granger causal connectivity analysis *J. Neurosci. Methods* **186** 262–73

[37] Barnett L and Seth A K 2014 The MVGC multivariate Granger causality toolbox: A new approach to Granger-causal inference *J. Neurosci. Methods* **223** 50–68

[38] Song Y, Yao M, Kemprecos H, Byrne Á and Xiao Z 2019 Predictive Coding Models for Pain Perception *bioRxiv* **6056** 1–49

[39] Baliki M N, Mansour A R, Baria A T and Apkarian A V 2014 Functional reorganization of the default mode network across chronic pain conditions *PLoS One* **9** e106133

[40] Gram M, Erlenwein J, Petzke F, Falla D, Przemeck M, Emons M I, Reuster M, Olesen S S and Drewes A M 2017 The cortical responses to evoked clinical pain in patients with hip osteoarthritis *PLoS One* **12** 1–14

[41] Bliss T, Collingridge G, … B K-N R and 2016 U 2016 Synaptic plasticity in the anterior cingulate cortex in acute and chronic pain *Nat. Rev. Neurosci.* **17** 485–96

[42] Gross J, Schnitzler A, Timmermann L and Ploner M 2007 Gamma oscillations in human primary somatosensory cortex reflect pain perception *PLoS Biol.* **5** 1168–73

[43] Liu C C, Chien J H, Chang Y W, Kim J H, Anderson W S and Lenz F A 2015 Functional role of induced gamma oscillatory responses in processing noxious and innocuous sensory events in humans *Neuroscience* **310** 389–400

[44] Schulz E, May E S, Postorino M, Tiemann L, Nickel M M, Witkovsky V, Schmidt P, Gross J and Ploner M 2015 Prefrontal gamma oscillations encode tonic pain in humans *Cereb. Cortex* **25** 4407–14

[45] Pertin M, Gosselin R-D and Decosterd I 2012 The Spared Nerve Injury Model of Neuropathic Pain *Pain Research: Methods and Protocols* vol 851, ed Z D Luo (Springer Science) pp 205–12

[46] Baliki M, Calvo O, Chialvo D R and Apkarian A V 2005

Spared Nerve Injury Rats Exhibit Thermal Hyperalgesia on an Automated Operant Dynamic Thermal Escape Task *Mol. Pain* **1** 1744-8069-1–18

[47] Chang P C, Pollema-Mays S L, Centeno M V, Procissi D, Contini M, Baria A T, Martina M and Apkarian A V 2014 Role of nucleus accumbens in neuropathic pain: Linked multi-scale evidence in the rat transitioning to neuropathic pain *Pain* **155** 1128–39

[48] Rampil I J and Laster M J 1992 No Correlation between Quantitative Electroencephalographic Measurements and Movement Response to Noxious Stimuli during Isoflurane Anesthesia in Rats *Anesthesiology* **77** 920–5

[49] Van Den Broek P L C, Van Rijn C M, Van Egmond J, Coenen A M L and Booij L H D J 2006 An effective correlation dimension and burst suppression ratio of the EEG in rat. Correlation with sevoflurane induced anaesthetic depth *Eur. J. Anaesthesiol.* **23** 391–402